



HAL
open science

Widespread formation of intracellular calcium carbonates by the bloom-forming cyanobacterium *Microcystis*

Juliette Gaëtan, Sébastien Halary, Maxime Millet, Cécile Bernard, Charlotte Duval, Sahima Hamlaoui, Amandine Hecquet, Muriel Gugger, Benjamin Marie, Neha Mehta, et al.

► To cite this version:

Juliette Gaëtan, Sébastien Halary, Maxime Millet, Cécile Bernard, Charlotte Duval, et al.. Widespread formation of intracellular calcium carbonates by the bloom-forming cyanobacterium *Microcystis*. *Environmental Microbiology*, 2023, 25 (3), pp.751-765. 10.1111/1462-2920.16322 . hal-04069101

HAL Id: hal-04069101

<https://hal.sorbonne-universite.fr/hal-04069101v1>

Submitted on 14 Apr 2023

HAL is a multi-disciplinary open access archive for the deposit and dissemination of scientific research documents, whether they are published or not. The documents may come from teaching and research institutions in France or abroad, or from public or private research centers.

L'archive ouverte pluridisciplinaire **HAL**, est destinée au dépôt et à la diffusion de documents scientifiques de niveau recherche, publiés ou non, émanant des établissements d'enseignement et de recherche français ou étrangers, des laboratoires publics ou privés.

Widespread formation of intracellular calcium carbonates by the bloom-forming cyanobacterium *Microcystis*

Juliette Gaëtan^{1,2}, Sébastien Halary³, Maxime Millet¹, Cécile Bernard³, Charlotte Duval³, Sahima Hamlaoui³, Amandine Hecquet², Muriel Gugger⁴, Benjamin Marie³, Neha Mehta¹, David Moreira⁵, Fériel Skouri-Panet¹, Cynthia Travert¹, Elodie Duprat¹, Julie Leloup², Karim Benzerara¹

¹Sorbonne Université, Muséum National d'Histoire Naturelle, UMR CNRS-SU-MNHN 7590. Institut de Minéralogie, de Physique des Matériaux et de Cosmochimie (IMPMC), Paris, France

²Sorbonne Université, UMR 7618 CNRS-INRA-IRD-Paris 7-UPEC. Institut d'Ecologie et des Sciences de l'Environnement de Paris (iEES-Paris), Paris, France.

³Muséum National d'Histoire Naturelle, UMR 7245 CNRS-MNHN. Molécules de Communication et Adaptation des Microorganismes, Paris, France

⁴Institut Pasteur, Université Paris Cité, Collection of Cyanobacteria, Paris, France

⁵Unité d'Ecologie Systématique et Evolution, CNRS, Université Paris-Saclay, AgroParisTech, Gif-sur-Yvette, France

Corresponding author: karim.benzerara@sorbonne-universite.fr

Data availability statement: Materials described in the manuscript will be freely available upon publication of the manuscript to any researcher wishing to use them for non-commercial purposes. Genomes of the 26 PMC strains have been deposited in ncbi (BioProject ID: PRJNA888979). All other datasets generated and/or analyzed during the current study (SEM/TEM) are available in the Zenodo repository, (doi: to be submitted).

Competing Interests statement: The authors declare no competing interest. The authors declare no competing financial interest

Funding statement: This work was supported by the ATM MNHN BIOCHEMIST project and the Emergence CaCO₃ project of Sorbonne University. Maxime Millet's grant was

supported by the Agence Nationale de la Recherche (ANR PHOSTORE, ANR-19-CE01-0005). Juliette Gaëtan PhD grant was funded by the Learning Planet Institute and University Paris Cité grant Frontiers of Innovation in Research and Education.

Originality-Significance Statement

This work reports the discovery of the pervasiveness of intracellular calcium carbonate inclusions in the *Microcystis*, a biological trait that has not been reported before despite intensive research on this cyanobacterial genus. This trait may confer to these blooming bacteria some overlooked geochemical importance in Ca geochemical cycle

Abstract

The formation of intracellular amorphous calcium carbonates (iACC) has been recently observed in a few cultured strains of *Microcystis*, a potentially toxic bloom-forming cyanobacterium found worldwide in freshwater ecosystems. If iACC-forming *Microcystis* are abundant within blooms, they may represent a significant amount of particulate Ca. Here we investigate the significance of iACC biomineralization by *Microcystis*. First, the presence of iACC-forming *Microcystis* cells has been detected in several eutrophic lakes, indicating that this phenomenon occurs under environmental conditions. Second, some genotypic (presence/absence of *ccyA*, a marker gene of iACC biomineralization) and phenotypic (presence/absence of iACC) diversity have been detected within a collection of strains isolated from one single lake. This illustrates that this trait is frequent but also variable within *Microcystis* even at a single locality. Finally, one-third of publicly available genomes of *Microcystis* were shown to contain the *ccyA* gene, revealing a wide geographic and phylogenetic distribution within the genus. Overall, the present work shows that the formation of iACC by *Microcystis* is common under environmental conditions. While its biological function remains undetermined, this process should be further considered regarding the biology of *Microcystis* and implications on the Ca geochemical cycle in freshwater environments.

Introduction

A broad phylogenetic diversity of bacteria affiliated with Cyanobacteria, Alphaproteobacteria, and Gammaproteobacteria can form intracellular amorphous calcium carbonates (iACC) (1–3). Through this process, cells sequester significant amounts of calcium (Ca) and inorganic carbon (C) intracellularly (4,5). Currently, iACC have been formally identified by electron microscopy in more than 20 cyanobacteria affiliated with diverse genera, families, and orders, originating from environments such as soils, hot springs, and fresh or marine water bodies (3,5,6). While the precise molecular mechanisms of intracellular iACC biomineralization remain unclear, this process has been proved to occur even under chemical conditions that are thermodynamically not favorable to iACC precipitation (7). Therefore, it involves some energy cost for the cells that may relate to active intracellular sequestration of Ca within a dedicated intracellular compartment, the biochemical composition of which remains unknown (7,8). Consistently with this active sequestration of Ca, iACC-forming cyanobacteria tend to incorporate more Ca than other cyanobacteria under laboratory conditions (5,7). As a result, they substantially decrease the concentration of extracellular Ca in their growth medium (7). The function of iACC granules in cyanobacteria remains unknown but they have been hypothesized to serve as ballasts by dramatically increasing the buoyant density of the cells (9), or as a pH buffer during photosynthesis (10), or an inorganic C reservoir (11), these few hypotheses being not exclusive.

Based on these observations, it has been advocated that iACC biomineralization is genetically controlled. Accordingly, a recently identified gene family, named *ccyA*, was shown to be linked with iACC formation in cyanobacteria (3). While the precise function of this gene family remains to be determined, some genomic and genetic analyses support a pivotal role in iACC biomineralization. This gene was searched in 594 GenBank genome assemblies assigned to cyanobacteria (published before December 1st, 2017) (3). Among them, 27 genomes contained *ccyA*, and 12 were affiliated with the *Microcystis* genus. Eight of these *Microcystis* strains related to *ccyA*-containing genomes were cultured under standard laboratory conditions and further analyzed by electron microscopy, and 6 formed iACC. This first identification of iACC in *Microcystis* showed that this trait had been overlooked so far in an otherwise extensively studied cyanobacterium.

Microcystis is among the most common bloom-forming cyanobacteria in freshwater ecosystems worldwide, and some ecotypes are toxic for humans and wildlife (12). Several factors have been proposed to explain the ecological success of *Microcystis*. They include the high cellular efficiency in taking up nutrients and inorganic C (13,14) and their ability to migrate vertically owing to specialized gas vesicles and high-density intracellular formations (12,15–17). These factors may *a priori* influence or are influenced by the capability of some *Microcystis* ecotypes to form iACC. However, presently there is no assessment of the commonness of iACC formation by *Microcystis*. Thus, we have combined microscopy and genomic analyses to determine the importance of iACC biomineralization by *Microcystis*. First, we analyzed *Microcystis* cells *in situ* in several lakes experiencing blooms seasonally. Second, we studied the phenotypic and genotypic diversity regarding iACC formation in a collection of *Microcystis* strains isolated from a single lake. Finally, we assess the distribution of the capability to form iACC within the *Microcystis* genus by genomic analyses.

Experimental Procedures

Sampling sites

Surface water samples were collected at five distinct locations to assess the presence of iACC in diverse *Microcystis* populations (Table I; Fig. S1). All sampled water bodies are affected by human activity (18). The sites of Champs-sur-Marne, Verneuil-sur-Seine, Cergy-Pontoise, and Grande Paroisse, are recreational lakes located in the suburban area of Paris, Ile-de-France, and are known to have experienced recurrent episodes of cyanobacterial blooms, including *Microcystis* ones, over the recent years (19–22). Champs-Sur-Marne, Verneuil-sur-Seine, and Cergy-Pontoise recreational areas were former quarries of alluvial and sand sediments, which were flooded between the 1940s and 1980s. La Portiña reservoir in Spain was flooded in 1947, in a granitoid bedrock, and has been used as a water supply since then (22).

For the sites of Champs-sur-Marne, Verneuil-sur-Seine and Cergy-Pontoise, identification of *Microcystis* cells by light microscopy was conducted by the service “Expertises environnementales” at the MCAM research unit (MNHN) (Fig. S2). No identification by light

microscopy was conducted for La Portiña and Grande Paroisse and were recognized based on their characteristic morphology by scanning electron microscopy.

Table I. Name and localization of studied water bodies

Name	City	Country	GPS	Date of sample collection for electron microscopy analyses	Strains isolation and sequencing
Grosse Pierre Pond	Verneuil-Sur-Seine	France	48.991306, 1.970930	20/10/2021	No
Les Galets Pond	Cergy-Pontoise	France	49.025860, 2.048909	18/09/2020 and 20/07/2021	No
Champs-sur-Marne recreational area	Champs-Sur-Marne	France	48.863889, 2.598056	08/10/2018 and 22/10/2018	Yes
La Noue de Notre Dame Pond	Grande Paroisse	France	48.375313, 2.901146	25/01/2022	No
Juanon reservoir	Valence	France	45.394166, 5.031944	No observation	Yes
Portiña reservoir	Portiña	Spain	40.000674,-4.842435	31/12/2021	No

Cultures of cyanobacterial strains

For culture experiments, twenty-four strains of *Microcystis* spp. were selected from the Paris Museum Collection (PMC) (Table S-I). They all originated from the same recreational pond in Champs-Sur-Marne (Ile-de-France, France), and their sequenced genomes were of good quality (completeness > 95% or contamination < 5%). All strains corresponded to non-axenic single clones of *Microcystis*. For the observations shown in the present manuscript, all strains were grown in a standard Z8 medium (23), without agitation, at 25°C with an 18:8 (day/night) photoperiod and a light intensity of 10 $\mu\text{mol photon m}^{-2} \text{s}^{-1}$. Except for strains PMC 568.08 and PMC 569.08, the same conditions were also used for strain curation. For curation, strains PMC 568.08 and PMC 569.08 were grown at 18°C with a 13:11 photoperiod (day/night) and a light intensity of 8 $\mu\text{mol photon m}^{-2} \text{s}^{-1}$.

Scanning electron microscopy (SEM)

Sample preparation for SEM was performed following a protocol previously tested on several iACC-forming strains, as described by (5,9). Briefly, cell suspensions from laboratory cultures and field water samples were filtered on 0.22 µm isopore polycarbonate filters, then rinsed three times with 10 mL MilliQ® water. Filters were air-dried at ambient temperature and mounted on aluminum stubs using double-sided carbon tape. It is well known that air-drying induces morphological artifacts such as cell shrinkage or cell-collapse. These artifacts are usually overcome by using techniques such as critical point drying. However, because of the use of chemicals, the latter approach induces iACC dissolution, whereas air-drying does not (9). Filters were coated by carbon evaporation to allow the conduction of electrons at the surface of samples for SEM analyses. SEM observations were performed using a Zeiss™Ultra55 SEM. The electron accelerating voltage was 10 or 15 kV with a working distance of 7.5 mm and a 60 µm aperture. Images were collected with a backscattered electron detector (AsB detector). Energy-dispersive X-ray spectrometry (EDXS) data were acquired using an EDS Bruker QUANTAX detector providing hyperspectral images (HyperMap), which were analyzed using the Esprit software (Bruker).

Scanning transmission electron microscopy (STEM)

Sample preparation for STEM was performed following a protocol previously tested on several iACC-forming strains, as described in (9,24). The cell pellets of *Microcystis* cultures were harvested by centrifugation (6600 g for 10 min) and then rinsed thrice with MilliQ® water. The cell pellets were re-suspended in 100-200 µL of MilliQ® water. A 3 to 6 µL aliquot was deposited on a carbon-coated 100- or 200-mesh copper grid and air-dried at ambient temperature. STEM analyses were performed using a JEOL-2100F microscope operated at 200 kV, equipped with a field emission gun, a JEOL detector, and a STEM device, which allows Z-contrast imaging in the high-angle annular dark field (HAADF) mode. Compositional mapping was acquired by performing EDXS analysis in the STEM-HAADF mode.

Genome sequencing and analyses

For genome sequencing, 28 strains of *Microcystis* spp. were selected from the Paris Museum Collection (PMC) including 25 originating from Champs-Sur-Marne (France), and

three isolated from another pond in Valence (France) (Table S-I and S-II). The 24 strains from Champs-sur-Marne used for cultures were among the 25 ones selected for genome sequencing. Strains were isolated as previously described (25). All strains were grown at 25°C for one month with a 16:8 photoperiod (day/night) and at a light intensity of 10-15 $\mu\text{mol photon m}^{-2} \text{s}^{-1}$. After centrifugation (3220 g for 15 min), the pellets were frozen at -80°C, then lyophilized for 24 h. DNA was extracted from 8 to 10 mg of biomass using the ZymoBIOMICS DNA Miniprep Kit (Zymo Research, CA) following the manufacturer's instructions, and sequenced using a 2x150 bp paired-reads strategy on an Illumina MiSeq platform.

Sequence datasets were corrected and assembled by SPAdes v3.12.0 (26) using default parameters, producing contigs belonging to *M. aeruginosa* or heterotrophic bacteria also present in the cultures. A synergistic approach allowed to extract sequences belonging to *M. aeruginosa* by (i) binning contigs using MyCC (27) based on several parameters, including sequence coverages obtained with bowtie2 (28), and (ii) taxonomic annotating using CAT (29). Two genomes (PMC 823.12 and PMC 729.11) were of poor quality (completeness < 95% or contamination > 5%) (Table S-I and S-II).

Additional genome assemblies belonging to the *Microcystis* genus were retrieved from the NCBI FTP server using both the genus name and children taxonomic identifiers of 1125 [*Microcystis*] on the 14th of January 2022. In total, 344 assemblies were collected from GenBank and/or RefSeq databases. Cross-references and assemblies belonging to the same strain were removed from the dataset, resulting in a final set of 278 assemblies. These assemblies were processed through CheckM to assess their quality (30) and Prodigal to predict their features when NCBI annotations were not available (29).

Search for *ccyA* in available genomes

The calcyanin protein, encoded by the *ccyA* gene, has been shown to be composed of two domains: a variable N-terminal domain and a conserved C-terminal domain (3). The conserved C-terminal domain of the 35 calcyanin protein sequences previously identified in cyanobacterial genomes was searched against the 256 genomes *Microcystis* assemblies showing a good quality (completeness > 95% and contamination < 5%) using the corresponding generated HMM profile (3) and the hmmsearch tool from HMMER (31). The sequence hits

matching the profile with coverage greater than 62% and an *E*-value lower than $1e-30$ were finely annotated using 3 HMM profiles corresponding to the 3 different GlyZip motifs that compose the complete C-terminal domain of the calcyanin protein. The N-terminal domain family of each full-length calcyanin was annotated using the BLASTp program. The 35 known *ccyA* N-terminal domains were used as a database. Overall, the hits were retained if they showed a complete C-terminal domain and a match against a known N-terminal domain with a minimum coverage of 80% (*E*-value $< 1e-7$). In addition, the retained sequences were searched in all *Microcystis* genomes using tBLASTn.

Phylogenetic analyses

A core genome consisting of 80 single-copy genes shared by (i) the 28 newly sequenced PMC *Microcystis* genomes, (ii) the 278 non-redundant publicly available *Microcystis* genome assemblies, and (iii) two outgroups (*Chroococcus* sp. FPU101 and *Merismopedia glauca* CCAP 1448/3) was retrieved using Roary (32) (minimal identity $\geq 80\%$). The concatenated gene sequences were aligned using MAFFT v7.453 (33) and used to infer a phylogenetic tree using RaxML v8.2.12 (34) (GTRGAMMA model, 100 bootstraps). Out of the analyzed 306 genomes, 282 (256 retrieved from the NCBI FTP server and 26 newly sequenced genomes from PMC collection) were of good quality (completeness $> 95\%$ and contamination $< 5\%$) and kept for this analysis. The phylogenetic tree was displayed and annotated using iTOL (35).

Results

Detection of iACC-forming *Microcystis* in lakes

Cell clusters with typical *Microcystis* morphology were detected based on light microscopy and/or electron microscopy in the five lakes (Ile-de-France and Toledo-Spain) known to recurrently experience cyanobacterial blooms (Fig. 1, 2, S2-S4). Cells were systematically imaged by SEM (Fig. 1). In all five lakes, many *Microcystis* cells contained intracellular inclusions, from a dozen (Fig. 1K-L) up to ~ 50 inclusions per cell (Fig. 1T). Their elemental composition was determined using energy-dispersive X-ray spectrometry (EDXS). Two types of inclusions were identified: (i) inclusions of the first type were composed of P as the major element, with some Mg, K, and sometimes Ca, and were interpreted as polyphosphate

granules (PolyP) (Fig. 1C and 1E); (ii) the other type of inclusions were rich in Ca and contained little to no P (Fig. 1C and 1D), which is characteristic of iACC inclusions in cyanobacteria (5,7,24). iACC inclusions were observed in *Microcystis* cells from all five lakes. In several samples, the distribution of iACC inclusions in cells was heterogeneous: for example, in La Portiña, within the same *Microcystis* cell cluster, both cells with numerous iACC inclusions (Fig. 2A, B, circle 2) and cells with only a few or no inclusion at all (Fig. 2A, B, circle 1) were observed. Finally, among cells with intracellular inclusions, some cells contained both PolyP and iACC (Fig. 1A-C, F-H and S-U; Fig. 3), some contained PolyP only (Fig. 4), and a few contained iACC inclusions only (Fig. 1 K-M and O-Q; Fig. 2).

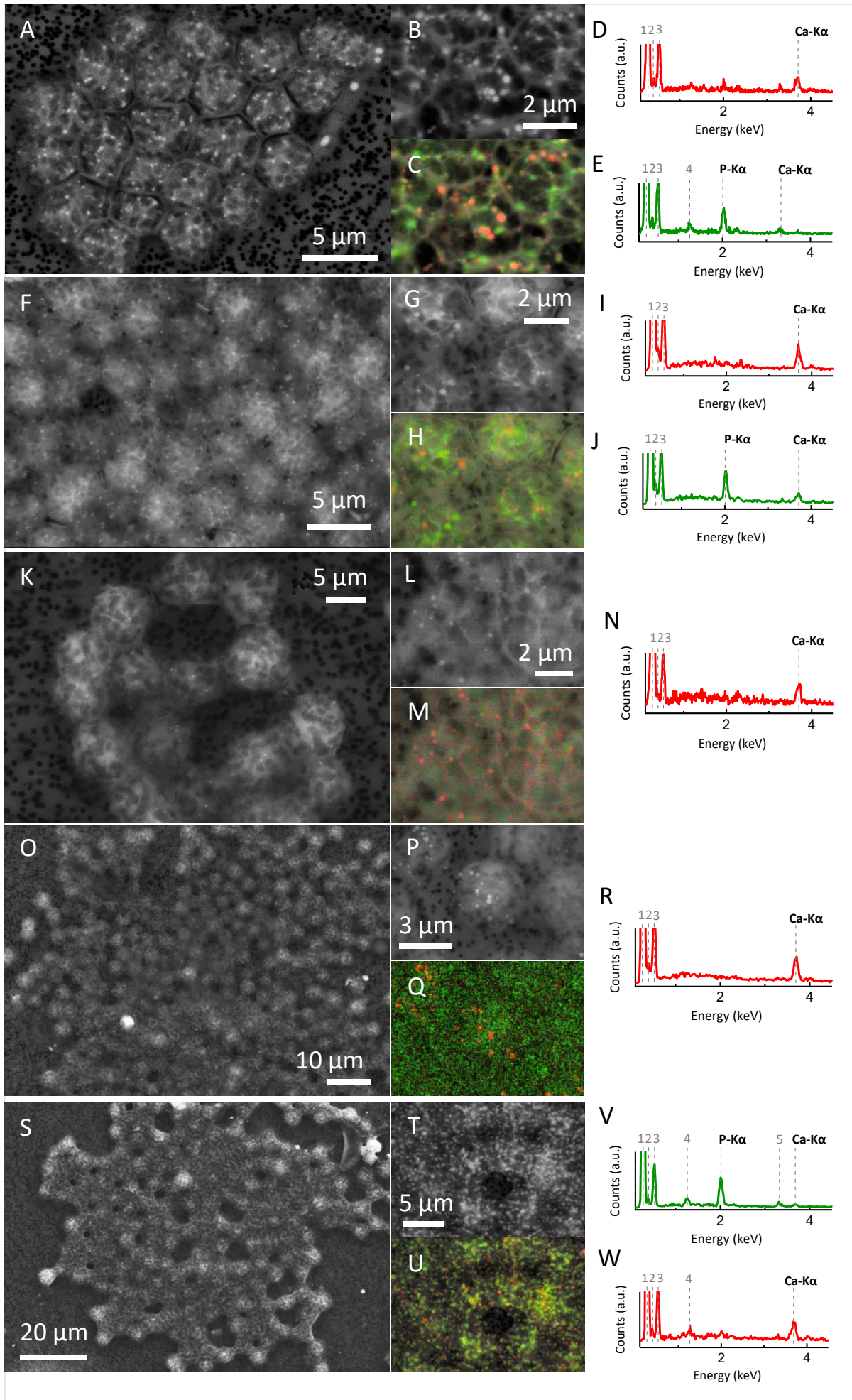


Figure 1: SEM analyses of Microcystis forming iACC and PolyP granules in freshwater lakes. (A-E): SEM image in AsB detection mode of *Microcystis* cells observed in samples from Champs-Sur-Marne (IdF-France). SEM images in AsB detection mode of a close-up view of the *Microcystis* cells. Corresponding overlay of the AsB image and SEM-EDX maps of Ca (red) and P (green). As a result, iACC appear in red and PolyP granules in green. EDXS spectra of iACC granules (red spots) and PolyP granules (green spots). (F-J): same type data for Verneuil (IdF-France). (K-N): same type of data for Cergy-Pontoise (IdF-France) with only an EDXS spectrum of iACC. (O-R): same type of data for Portiña (Toledo – Spain) with only an EDXS spectrum of iACC. (S-W): same type of data for Grande Paroisse (IdF-France). The labels of the emission lines in the EDXS spectra are: (1) C K α ; (2) N K α ; (3) O K α ; (4) Mg K α ; (5) K K α .

Detection of both iACC and the *ccyA* gene in cultivated *Microcystis* strains isolated from a single lake

Twenty-four *Microcystis* spp. strains isolated from the Champs-Sur-Marne lake (France) were investigated for their phenotypic and genotypic diversity (Table S-I). Two strains were isolated in 2008, while the 22 others were isolated in August 2011 (18 strains) and in October 2011 (4 strains). Electron microscopy analyses showed that all strains contained PolyP inclusions, which can be morphologically but not chemically confused with iACC inclusions (Fig. 5, Fig. S3 and S4). By contrast, iACC inclusions were detected only in the cells of 7 strains by SEM and SEM-EDX analyses, as indicated by their relatively high contrast, high Ca content, and negligible P content (Fig. S4). SEM analyses for the PMC 820.12 and PMC 831.12 strains were more ambiguous. Indeed, a Ca signal could be detected in the spectra obtained on the whole cells, but it was difficult to spatially discriminate from the P signal. Therefore, these two strains were further analyzed by STEM-HAADF, which provides a higher spatial resolution than SEM. This unambiguously showed that these two strains contained iACC (Fig. 5 A-D and H-K). Overall, electron microscopy revealed that 9 out of 24 strains (37.5%) contain iACC.

In parallel, the genomes of these 24 strains were sequenced and used to search for the *ccyA* gene. This gene was detected in all 9 strains forming iACC, and was absent from the genomes of the 15 other strains. Moreover, the N-terminal domains of all the calcyanins belonged to the same homologous family (sharing at least 88.3% identity between their amino acids sequences) corresponding to the one (named Z-type) previously identified for *Microcystis* (3).

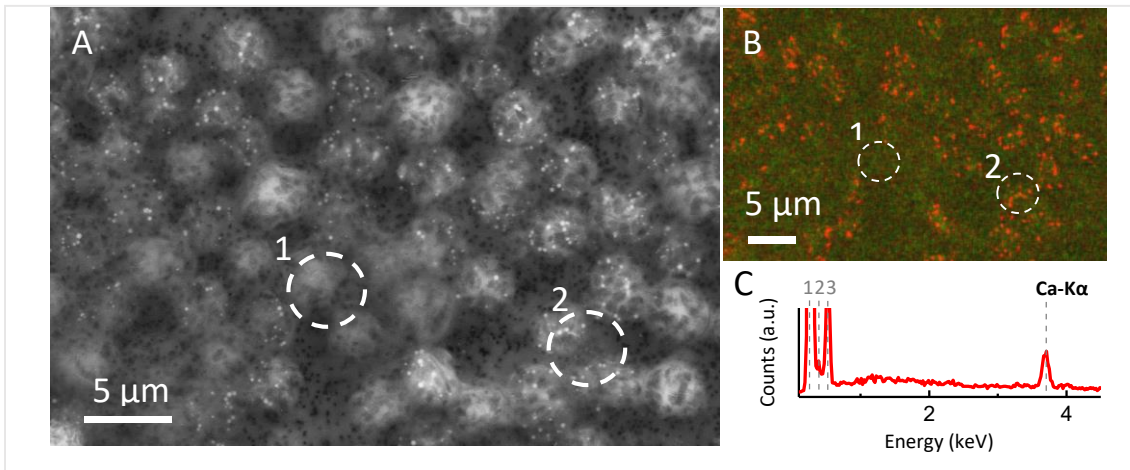


Figure 2: SEM analyses of *Microcystis* cells from La Portiña with some cells containing iACC inclusions and some not containing iACC. (A) SEM image in AsB detection mode of a group of *Microcystis* cells collected from La Portiña (Toledo-Spain). (B) Overlay of AsB image and SEM-EDX maps of Ca (red) and P (green). As a result, iACC appear in red. (C) EDXS spectrum of iACC granules (red spots) shown in circle 2 in B. The labels of the emission lines in the EDXS spectra are the same as in Fig. 1.

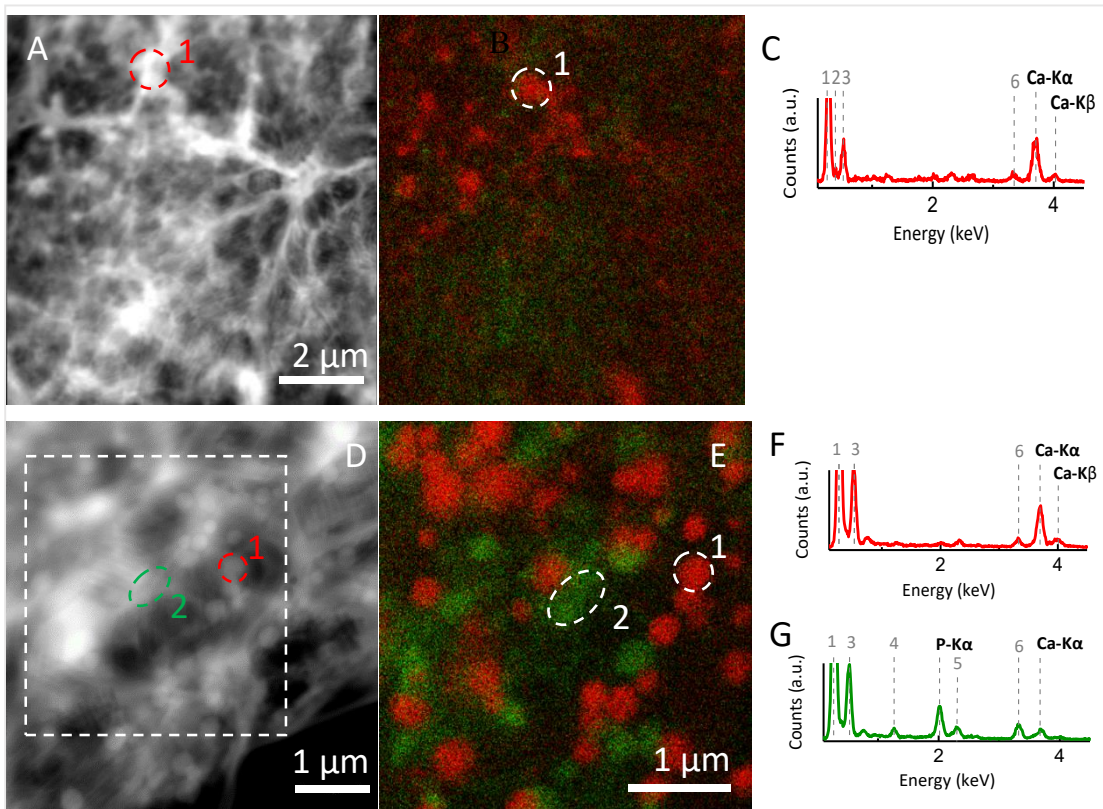


Figure 3: TEM analyses of *Microcystis* cells forming iACC and PolyP granules collected in freshwater lakes. (A): STEM-HAADF image of *Microcystis* cells observed in Champs-Sur-Marne (IdF-France). (B): Corresponding STEM-EDX map of Ca (red) and P (green). iACC inclusions appear in red and PolyP granules in green. (C): EDXS spectrum acquired on the iACC inclusion outlined in (B). (D-G): same analyses on *Microcystis* cells collected in Cergy-Pontoise. The labels of the emission lines in the EDXS spectra are (4) Mg K α ; (5) S K α ; (6): K K α .

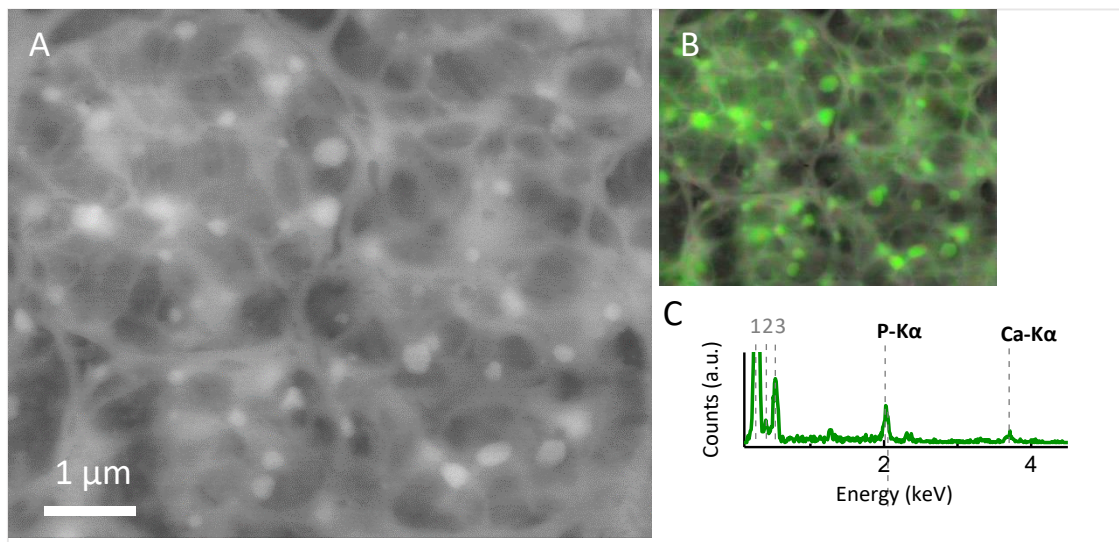


Figure 4: SEM analyses of *Microcystis* cells forming PolyP only. (A) SEM image taken in the AsB detection mode of a cluster of *Microcystis* cells observed in the Cergy-Pontoise lake. (B) Overlay of AsB image and SEM-EDX maps of Ca (red) and P (green). As a result, PolyP granules appear in green. (C) EDXS spectrum of green spots shown in B.

Search for full-length homologs of the *ccyA* gene in *Microcystis* genomes from public databases

To go further, 256 complete genome assemblies of high quality affiliated with the *Microcystis* genus were retrieved from the curated NCBI genomic databases. Twenty-six newly sequenced genomes of *Microcystis* PMC strains were added to this dataset: the above-described 24 genomes of strains isolated from Champs-Sur-Marne, and two additional genomes of strains from Valence, France. Overall, the *ccyA* gene was found in 93 out of the 282 *Microcystis* genomes assemblies (Table S-I). The *ccyA* gene was present in single copy in all genomes where it was detected. Among these 93 *ccyA*⁺ genomes, 84 were already in NCBI databases and nine belonged to our newly sequenced genomes of PMC strains. All these *ccyA* sequences were well conserved (sharing at least 72.6% identity) and their N-terminal domain all belong to the same Z-type family.

The obtained *ccyA* dataset contained sequences from both cultured strains and metagenome-assembled genomes (MAGs), the latter representing a significant number of available *Microcystis* genomes (148 out of the 282 genomes; 38 *ccyA*⁺ MAGs out of the identified 93 *ccyA*⁺ genomes) (Table S-I). Moreover, *ccyA*⁺ genotypes were recovered from multiple geographic locations, spanning 12 different countries over five continents (Asia,

Europe, Africa, and North and South America), showing the cosmopolitanism of this gene. This considerably extends the assessment of *ccyA* distribution in the *Microcystis* genus compared with the 12 *Microcystis ccyA+*-genomes that were known up to now (3).

To better assess the link between phylogeny and the distribution of *ccyA* in *Microcystis*, a phylogenomic tree was built based on a core genome composed of 80 single-copy genes (Fig. 6). Several genotypic groups, previously defined by Pérez-Carrascal *et al.* (2019) (36) and modified by Dick *et al.* (2021) (37), based on the 16S-23S internal transcribed spacer (ITS), are reported in our analysis (Fig. 6). Except for the Mae 3_3 genotypic group, which is inserted within the Mae 3_2 group in this study, all other genotypic groups were recovered in our phylogenomic analysis. Moreover, all the newly sequenced PMC strains, except one (PMC 568), were closely related to four existing genotypic groups: four strains within Mae 4, 13 within Mae 8, seven within Mae 7, and one within the Mae 3_1 cluster.

To better assess the link between geography and the distribution of *ccyA* within *Microcystis*, a total of 16 geographic groups (*i.e.*, sets of at least 3 good-quality genomes of organisms isolated from a given geographic location, at the same time period) were defined (Table S-III). These groups were broadly distributed across the phylogenetic tree. Seven geographic groups (geographic groups 3, 5, 6, 7, 9, 15 and 16) contained both *ccyA+* and *ccyA-* genomes, one (geographic group 11) contained *ccyA+* genomes only, and the other seven (geographic groups 1, 2, 4, 8, 10, 13 and 14) contained *ccyA-* genomes only. Interestingly, while most of these groups contained less than 10 genomes, four comprised more than 25 genomes. One group, geographic group 7, comprised 26 genomes sequenced during a bloom event in 2018 (Lake Pampulha, Brazil) and was mostly composed of *ccyA+* genomes (23 over 26). Two other large groups of genomes (geographic groups 13 and 14) were retrieved from Lake Champlain (Canada) in 2017 and 2018. They comprise 41 and 32 high-quality genome assemblies, respectively, none containing *ccyA*. In contrast with these three large geographic groups, which had a pronounced bias towards *ccyA+* or *ccyA-*, the one identified in Champs-sur-Marne (geographic group 17) showed similar proportions of *ccyA+* and *ccyA-* genomes.

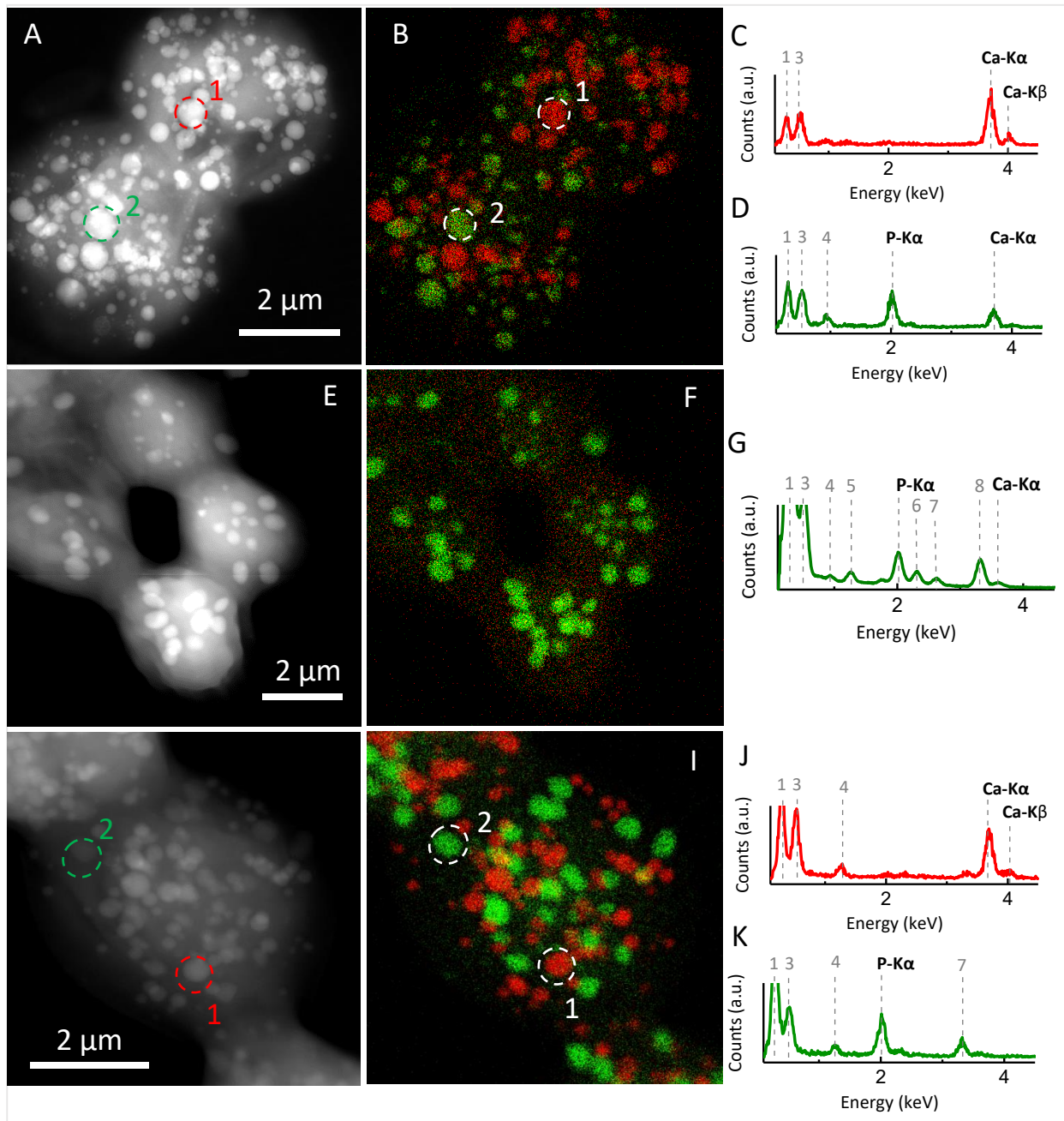


Figure 5: TEM analyses of *Microcystis* cultured strains. (A-D): STEM-HAADF image of two cells of *Microcystis* PMC 831.12, which form both iACC and PolyP granules; corresponding STEM-EDX maps of Ca (red) and P (green). As a result, iACC granules appear in red and PolyP granules in green; EDXS spectra measured on the iACC and PolyP granules outlined in A and B. (E-G): same data for cells of *Microcystis* PMC 813.12, which form PolyP granules only. The labels of the emission lines in the EDXS spectra are: (1): C K α ; (3) O K α ; (4) Na K α ; (5) Mg K α ; (6): S K α ; (7): Cl K α ; (8): K K α . (H-K): same data for cells of *Microcystis* PMC 820.12, which form both iACC and PolyP granules.

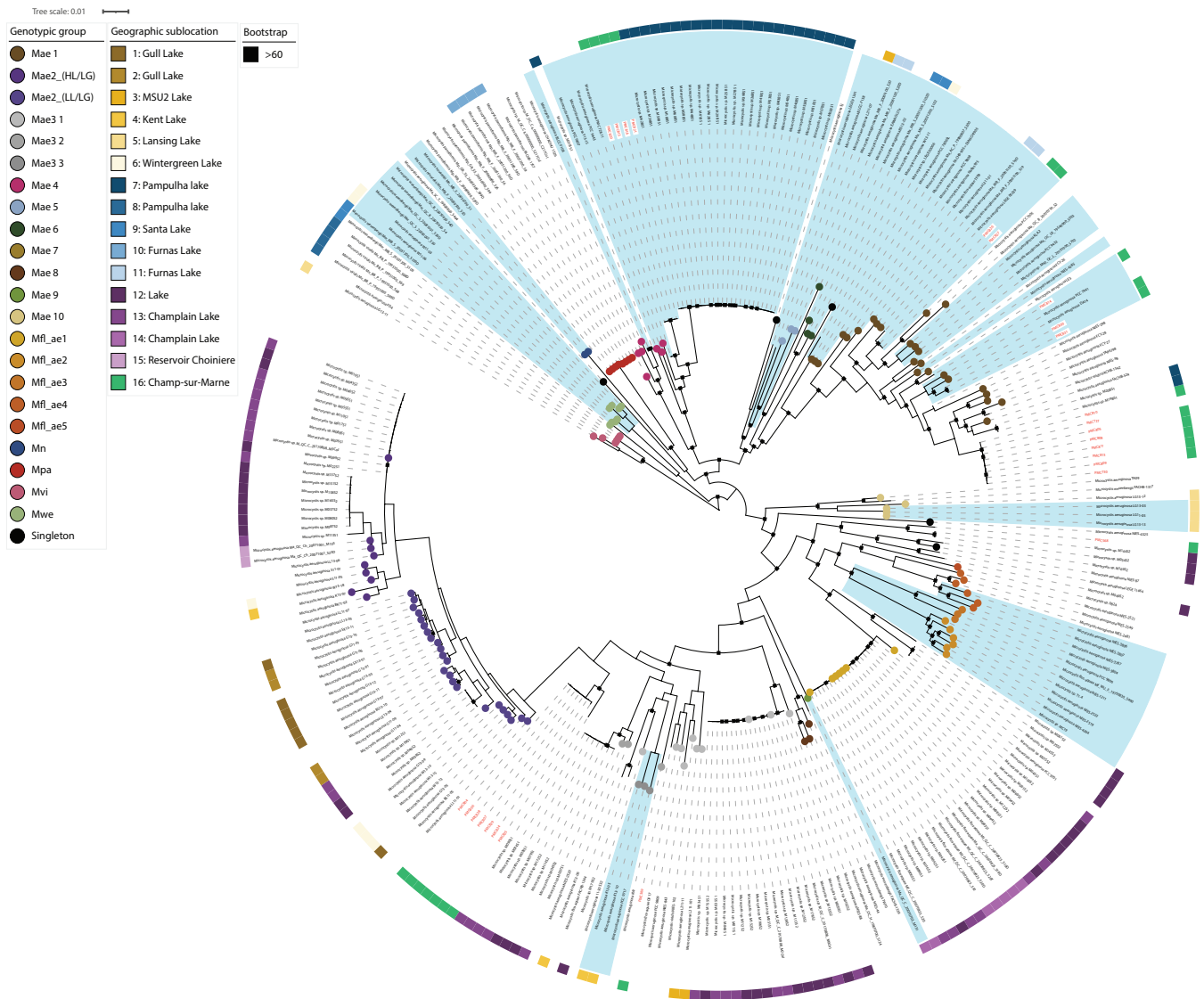


Figure 6: Phylogenomic tree of *Microcystis*. The colored outer ring indicates the geographic sublocation of the genomes based on their geographic origin and time of isolation (Table S-III); see color code on the figure. Genomic assemblies containing the *ccyA* gene are shadowed in blue. Colored circles at the tips of the tree branches indicate genotypic groups as defined in the literature; see color code on the figure. Nodes with a bootstrap value over 60% are represented as filled black squares.

Discussion

The overlooked prevalence of iACC biomineralization by *Microcystis*

This study shows that the formation of iACC by *Microcystis* is very common. It may seem surprising that this trait was not described before, considering the numerous past

observations of *Microcystis* blooms. Recently, Benzerara et al. (2022) reported the detection of (i) the *ccyA* gene, a reliable marker of iACC biomineralization, in 12 *Microcystis* genome assemblies and (ii) iACC in 6 of the corresponding *Microcystis* strains that could be observed, all coming from the Pasteur Culture Collection of Cyanobacteria (PCC). Here, we observed iACC in 9 out of 24 strains from the Paris Museum Collection (PMC) and identified 93 genomes of *Microcystis* containing the *ccyA* gene, retrieved from all around the world. These results significantly extend the prevalence of iACC biomineralization by *Microcystis* and confirm the strong correlation between the presence of *ccyA* and the formation of iACC: this correlation was perfect for the 24 PMC strains from Champs-Sur-Marne. This strongly supports the premise that iACC biomineralization capabilities can be predicted in *Microcystis* strains based on the presence/absence of the *ccyA* gene. Yet, it should be noted that despite the robustness of this correlation, few ‘false positives’ cases were reported by Benzerara *et al.* (2022), *i.e.* strains harboring *ccyA* but in which iACC was not detected in laboratory cultures. These false positives are two axenic *Microcystis* PCC strains (*M. aeruginosa* PCC 9432 and PCC 9717, belonging to the genotypic groups Mae1 and Mae3_3, respectively). It was proposed that the tested culture conditions might not always promote iACC formation within these strains or that one or more of the other to-be-identified genes involved in the biomineralization process might be missing. Therefore, the proportion of 93 genomes with *ccyA* out of 282 good-quality genomes (~1/3) should be considered as an overestimated proportion of iACC-forming strains. Future systematic microscopy analyses of strains with sequenced genomes may allow refining this ratio.

The iACC inclusions are not only detected in cultures but also in samples from five freshwater lakes. This illustrates that iACC biomineralization is not restricted to laboratory conditions but also occurs under environmental conditions. Multiple reasons may explain why this common feature has been overlooked in the past: (i) a strong or total loss of iACC has been reported upon several sample preparation protocols, including those involving the use of chemical fixatives, such as in standard ultramicrotomy (9,38); (ii) cells degrade rapidly under the electron beam, which complicates the imaging of iACC inclusions, especially when they are relatively small; (iii) iACC inclusions can be confused with other types of inclusions such as PolyP, which therefore requires to conduct spatially resolved chemical analyses (e.g., by SEM- or STEM-EDXS). Electron microscopy analyses can be fastidious to conduct on multiple

samples and do not easily provide a statistically accurate assessment of the proportion of iACC-forming *Microcystis* cells in a population where both *ccyA*- and *ccyA*+ are present, such as in Champs-sur-Marne. However, this assessment may be more straightforward by genomic approaches in populations where mostly *ccyA*+ genomes are detected. In the future, the use of bulk analyses such as Fourier transform infrared (FTIR) spectroscopy, sensitive enough to iACC within cyanobacterial cells may help to more rapidly screen large amounts of samples as recently shown by Mehta *et al.* (2022) (39).

Potential impacts on the Ca geochemical cycle

Some geochemical implications of the evidenced prevalence of iACC biomineralization by *Microcystis* can be explored. Recent studies (5,7) assessed that iACC+ cyanobacteria (based on analyses of several genera but *Microcystis*) may contain from ~10 to 185 mg of Ca per g of dry matter. The dry biomass of *Microcystis* blooms can reach up to 3,5 mg.L⁻¹ (40). Assuming that the Ca amounts per cell previously estimated can be applied to *Microcystis*, the Ca content of the cells during a bloom event would be equivalent to a Ca concentration from 0.87 μM to 16.2 μM if all Ca from iACC was released to the extracellular solution in the depth band where the aforementioned cell density is achieved. This is significant when compared to the range (10 μM and 1800 μM) of dissolved Ca concentrations in continental aqueous environments (41). Overall, this shows that iACC within *Microcystis* may represent a significant reservoir of the Ca geochemical cycle in lakes during blooms. Similarly, based on the same numbers, iACC in a *Microcystis* bloom may be equivalent to 0.87 μM to 16.2 μM of inorganic carbon. This may appear more modest compared to the ~0.15 μM to 7 mM range of dissolved inorganic carbon detected in continental aqueous environments (41). However, there are strong diurnal fluctuations due photosynthetic uptake, and high temperatures might lower the concentrations due to the lower solubility of CO₂ and overall, future studies should be conducted to better assess the potential importance of iACC as an inorganic carbon reservoir.

Moreover, De Wever *et al.* (2019) showed a better growth of some iACC+ cyanobacteria at higher Ca concentrations. However, this was not the case for all iACC+ cyanobacteria and we do not currently know if this is the case for *Microcystis* strains. Yet, if this is true for *Microcystis* as well, a negative feedback loop may occur: the onset of massive iACC+ *Microcystis* blooms may result in a decrease of extracellular dissolved Ca

concentrations. This decrease may subsequently induce a limitation of iACC+ *Microcystis* growth. Interestingly, the role of Ca in *Microcystis* ecology has been already mentioned in the past, since it has been suggested that high concentrations of Ca (> 2.5 mM) may promote the formation of blooms (42,43). Here, we speculate that Ca has an additional role, i.e. feeding the formation of iACC, at least for some *Microcystis* genotypes/phenotypes biomineralizing iACC.

Phylogenetic distribution of *ccyA*

In the present study, our phylogenomic analysis has found most of the 22 genotypic groups defined by Pérez-Carrascal *et al.* (2019) and modified by Dick *et al.* (2021). However, it is important to note that some nodes remain poorly supported (bootstrap values below 60%), which nuances the relative positioning of these clusters. The *ccyA* gene is found in 12 different genotypic groups (Mwe, Mn, Mae 4, Mae 5, Mae 6, Mae 8 to 10, Mfl ae 2 to 4, and Mae3 2), showing that *ccyA*, and thus potentially the ability to form iACC, is widespread within the *Microcystis* genus. The number of available genomes belonging to those genotypic groups widely differs. For example, the Mae2_(HL/LG) group has an especially large number of representative genomes, which might be due to a greater sampling effort. Because of the heterogeneous distribution of *ccyA* among genotypic groups, the biased sampling of these groups may directly induce a bias in the proportion of *ccyA*+/*ccyA*- genomes.

Genomes containing the *ccyA* gene distribute as relatively large clusters in the phylogenetic tree of *Microcystis*. In particular, several clusters stretch over most of the top part of the tree shown in Figure 6, extending from *Microcystis aeruginosa* LG13-11 to PMC 730, with most genomes possessing the *ccyA* gene. Few other clusters span the rest of the tree, dispersed in between genomes not possessing the gene. As previously suggested by Benzerara *et al.* (2022), the distribution of *ccyA* in the cyanobacteria phylogenetic tree was best explained by vertical transfers of *ccyA* from an ancient ancestor to modern cyanobacteria with multiple independent losses. Assuming that this is also true at the scale of the *Microcystis* genus, one can explain the distribution of *ccyA* in the “top” part of the tree by at most 10 gene loss events, this estimation being probably overestimated due to the weak support of some of these nodes. Consistently, loss events have been shown to be frequent in *Microcystis* (44,45). Moreover, families of genes that were shown to contract over evolutionary time scales were enriched, notably in the function of “inorganic ion transport and metabolism” (45). The “bottom” part of

the tree with few *ccyA* occurrences can be most parsimoniously explained by one ancient loss of *ccyA* followed by few secondary (re)gains by horizontal gene transfers (HGT) (e.g. for the Mae 3_3 group). HGT is recurrently described as a frequent process in *Microcystis* genus (45–47), which may support this explanation.

***Microcystis* within-population diversity based on *ccyA* presence/absence**

Overall, *ccyA* appears as an accessory gene in *Microcystis*, since it is present in 93 out of 282 good-quality genomes. Therefore, it adds to the striking diversity of dispensable genes (i.e. accessory genes and unique genes) found in the highly plastic genome of *Microcystis* (45,46,48), that are involved in various functions such as replication, recombination, repair, signal transduction, and transcription (48), or the extensively studied function of toxin production (49). However, a significant part of the accessory genes, such as *ccyA*, lacks functional annotation. It has been advocated that this open pangenome and the strain-level genomic diversity could have a key role in the ecological success of *Microcystis*, by offering an efficient strategy to quickly adapt to a fluctuating environment, with the dominance of certain phenotypes within a mixed population or under local conditions (37,50). Based on these general considerations, the *ccyA* gene may provide some ecological success under some particular environmental conditions that remain to be determined. Whether these conditions may be related with calcium and/or inorganic carbon availability and whether this availability might fluctuate over time remains to be studied. One way to assess these conditions may consist in determining the relationship between genotypic diversity and environmental conditions. We identified four geographic groups large enough so that the within-population micro-diversity of *Microcystis* can be assessed. Three were dominated by either *ccyA*⁺ (one from Lake Pampulha) or *ccyA*⁻ (two from Lake Champlain) genomes. By contrast, the Champs-sur-Marne geographic group contained both *ccyA*⁺ and *ccyA*⁻ genomes at the same time during a bloom. The *ccyA*⁺ strains in the Pampulha dataset affiliated with one genetic cluster only, suggesting some possible dominance of the bloom population by one *ccyA*⁺ clone. In Champs-sur-Marne, *ccyA*⁺ strains affiliated with 2 different genotypic groups. Overall, these particular distributions of *ccyA* within *Microcystis* populations suggest that some yet-to-identify biotic and abiotic parameters of the ecosystems may favor the dominance or absence of iACC-forming strains in environments such as Lake Pampulha or Lake Champlain. Yet, based on this assumption, the

presence of both *ccyA* +/- genotypes at the same date, co-existing spatially in ecosystems such as in Champs sur Marne is more intriguing. It is important to consider that, unlike the Lake Pampulha and Lake Champlain groups, the genomes retrieved from Champs sur Marne were obtained from cultures, and this could influence the *ccyA*+/*ccyA*- ratio of this group. Indeed, assessing genotypic diversity in an environment using cultivation-based samples is difficult, since strains better adapted to the high concentration of nutrients typically found in culture media compared with the environmental conditions are preferentially selected (49). Alternatively, such a genotypic diversity in a single population may really occur similarly to what was evidenced before (51,52). Among other possible explanations, the existence of some local variable ecological niches was suggested. Alternatively, one may hypothesize a temporal dynamic of *ccyA*+ genotypes paralleling the bloom dynamics. These dynamics are associated with strong variations of, e.g., pH, N, P, and pCO₂ concentrations, which are parameters known to favor the emergence of specific genotypes and shifts within *Microcystis* populations (36,43). At some moments, when shifts take place, one may expect mixtures of different genotypes.

The *ccyA* gene is highly conserved among the *Microcystis* genus ($\geq 72.6\%$ identity). If it has not been horizontally transferred recurrently among the different *Microcystis* lineages, this suggests that there is a strong selective pressure, and thus some functional importance of calcyanin for the cell. So far, some potential functions have been speculated for iACC, including intracellular pH buffering, a reserve of inorganic carbon, or a ballast (53). How such functions may relate to environmental parameters such as dissolved Ca concentrations, variability of the inorganic C availability, and/or pH variations are not clear. Unfortunately, those parameters are not routinely monitored. Future temporal studies will help to pinpoint and explore further the correlations between these abiotic parameters and the co-dominance of *ccyA*+ or *ccyA*- genotypes in *Microcystis* populations. Moreover, it can be hypothesized that iACC formation is related with carbon concentrating mechanisms (CCM), which have been abundantly described in cyanobacteria (e.g., 54). However, this currently remains an uncharted topic and future studies may dwell on the present one to test if some genes involved in CCM might be differentially expressed in *ccyA*+ or *ccyA*- strains. Similarly, although first quick observations do not suggest it, the existence of a potential correlation between strain toxicity and iACC formation should be tested in the future. Last, genetic studies may help to unravel if

the deletion of the *ccyA* gene may have some additional effect on cells than formation of iACC only.

Conclusions

Overall, our study shows that the biomineralization of iACC is a common trait in *Microcystis*, under laboratory conditions as well as under environmental conditions. The correlation between the capability to form iACC and the presence of the *ccyA* gene as suggested by Benzerara et al. (2022) is further supported by combined electron microscopy and genomic analyses of 24 newly sequenced *Microcystis* genomes. This marker gene is an accessory gene in the *Microcystis* pangenome. Its quasi-binary distribution (i.e., either all *ccyA*⁺ or *ccyA*⁻) in some extensive datasets suggests that some not-yet-identified environmental parameters may favor *ccyA*⁺ or *ccyA*⁻ genotypes. Blooming populations of *ccyA*⁺ *Microcystis* may significantly impact the geochemical cycle of Ca, a hypothesis that will be further tested in future studies.

Acknowledgments

We thank Baptiste Ancieaux, Fabien Franc and Mehdi Mokhtari from the Île de Loisirs of Cergy and Jeton Maksutaj and Pierre Wunen-Burger from the Nautical centre Val-de-Seine for their help. We thank Imène Estève, Béatrice Doisneau and Stéphanie Delbrel from the SEM platform at IMPMC, as well as Jean-Michel Guigner from the IMPMC TEM platform.

References

1. Monteil CL, Benzerara K, Menguy N, Bidaud C, Michot-Achdjian E, Bolzoni R, et al. Intracellular amorphous Ca-carbonate and magnetite biomineralization by a magnetotactic bacterium affiliated to the Alphaproteobacteria. *ISME J.* 2021;15(1):1–18.
2. Benzerara K, Bolzoni R, Monteil C, Beyssac O, Forni O, Alonso B, et al. The gammaproteobacterium *Achromatium* forms intracellular amorphous calcium carbonate and not (crystalline) calcite. *Geobiology.* 2021;19(2):199–213.

3. Benzerara K, Duprat E, Bitard-Feildel T, Caumes G, Cassier-Chauvat C, Chauvat F, et al. A New Gene Family Diagnostic for Intracellular Biomineralization of Amorphous Ca Carbonates by Cyanobacteria. Dagan T, editor. *Genome Biol Evol.* 2022;14(3):evac026.
4. Gray N, Head I. The Family Achromatiaceae. In: Rosenberg E, DeLong EF, Lory S, Stackebrandt E, Thompson F, editors. *The Prokaryotes*. Berlin, Heidelberg: Springer; 2014;p.1–14.
5. Wever AD, Benzerara K, Coutaud M, Caumes G, Poinot M, Skouri-Panet F, et al. Evidence of high Ca uptake by cyanobacteria forming intracellular CaCO₃ and impact on their growth. *Geobiology*. 2019;17(6):676–90.
6. Ragon M, Benzerara K, Moreira D, Tavera R, Lopez-Garcia P. 16S rDNA-based analysis reveals cosmopolitan occurrence but limited diversity of two cyanobacterial lineages with contrasted patterns of intracellular carbonate mineralization. *Front Microbiol.* 2014;5.
7. Cam N, Benzerara K, Georgelin T, Jaber M, Lambert JF, Poinot M, et al. Cyanobacterial formation of intracellular Ca-carbonates in undersaturated solutions. *Geobiology*. 2018;16(1):49–61.
8. Blondeau M, Sachse M, Boulogne C, Gillet C, Guigner JM, Skouri-Panet F, et al. Amorphous Calcium Carbonate Granules Form Within an Intracellular Compartment in Calcifying Cyanobacteria. *Front Microbiol.* 2018;9:1768.
9. Li J, Margaret Oliver I, Cam N, Boudier T, Blondeau M, Leroy E, et al. Biomineralization Patterns of Intracellular Carbonatogenesis in Cyanobacteria: Molecular Hypotheses. *Minerals*. 2016;6(1):10.
10. Couradeau E, Benzerara K, Gérard E, Moreira D, Bernard S, Brown GE, et al. An Early-Branching Microbialite Cyanobacterium Forms Intracellular Carbonates. *Science*. 2012;27;336(6080):459–62.

11. Görden S, Benzerara K, Skouri-Panet F, Gugger M, Chauvat F, Cassier-Chauvat C. The diversity of molecular mechanisms of carbonate biomineralization by bacteria. *Discov Mater.* 2021;1(1):2.
12. Harke MJ, Steffen MM, Gobler CJ, Otten TG, Wilhelm SW, Wood SA, et al. A review of the global ecology, genomics, and biogeography of the toxic cyanobacterium, *Microcystis* spp. *Harmful Algae.* 2016;54:4–20.
13. Saxton MA, Arnold RJ, Bourbonniere RA, McKay RML, Wilhelm SW. Plasticity of Total and Intracellular Phosphorus Quotas in *Microcystis aeruginosa* Cultures and Lake Erie Algal Assemblages. *Front Microbiol.* 2012;3.
14. Wang Y, Wu M, Yu J, Zhang J, Zhang R, Zhang L, et al. Differences in growth, pigment composition and photosynthetic rates of two phenotypes *Microcystis aeruginosa* strains under high and low iron conditions. *Biochem Syst Ecol.* 2014;55:112–7.
15. Reynolds CS, Jaworski GHM, Cmiech HA, Leedale GF, Lund JWG. On the annual cycle of the blue-green alga *Microcystis Aeruginosa* Kütz. Emend. Elenkin. *Philos Trans R Soc Lond B Biol Sci.* 1981;293(1068):419–77.
16. Thomas RH, Walsby AE. Buoyancy Regulation in a Strain of *Microcystis*. *Microbiology.* 1985;131(4):799–809.
17. Gobler CJ, Burkholder JM, Davis TW, Harke MJ, Johengen T, Stow CA, et al. The dual role of nitrogen supply in controlling the growth and toxicity of cyanobacterial blooms. *Harmful Algae.* 2016;54:87–97.
18. Catherine A, Mouillot D, Escoffier N, Bernard C, Troussellier M. Cost effective prediction of the eutrophication status of lakes and reservoirs. *Freshw Biol.* 2010;55(11):2425–35.

19. Ledreux A, Thomazeau S, Catherine A, Duval C, Yéprémian C, Marie A, et al. Evidence for saxitoxins production by the cyanobacterium *Aphanizomenon gracile* in a French recreational water body. *Harmful Algae*. 2010;10(1):88–97.
20. Louati I, Pascault N, Debroas D, Bernard C, Humbert JF, Leloup J. Structural Diversity of Bacterial Communities Associated with Bloom-Forming Freshwater Cyanobacteria Differs According to the Cyanobacterial Genus. *PLOS ONE*. 2015;10(11):e0140614.
21. Sotton B, Paris A, Le Manach S, Blond A, Duval C, Qiao Q, et al. Specificity of the metabolic signatures of fish from cyanobacteria rich lakes. *Chemosphere*. 2019;226:183–91.
22. Vieira-Lanero R, Barca S, Cobo MC, Cobo F. Occurrence of Freshwater Cyanobacteria and Bloom Records in Spanish Reservoirs (1981–2017). *Hydrobiology*. 2022;1;1(1):122–36.
23. Kotai J. Instructions for preparation of modified nutrient solution Z8 for algae. 1972.
24. Benzerara K, Skouri-Panet F, Li J, Ferard C, Gugger M, Laurent T, et al. Intracellular Calcium carbonate biomineralization is widespread in cyanobacteria. *Proc Natl Acad Sci*. 2014;111(30):10933–8.
25. Halary S, Duval C, Gallet A, Duperron S, Piquet B, Demay J, et al. Draft Genome Sequence of the Toxic Freshwater *Microcystis aeruginosa* Strain PMC 728.11 (Cyanobacteria, Chroococcales). *Microbiol Resour Announc*. 2020;9(48):e01096-20.
26. Bankevich A, Nurk S, Antipov D, Gurevich AA, Dvorkin M, Kulikov AS, et al. SPAdes: A New Genome Assembly Algorithm and Its Applications to Single-Cell Sequencing. *J Comput Biol*. 2012;19(5):455–77.
27. Lin HH, Liao YC. Accurate binning of metagenomic contigs via automated clustering sequences using information of genomic signatures and marker genes. *Sci Rep*. 2016;6(1):24175.

28. Langmead B, Salzberg SL. Fast gapped-read alignment with Bowtie 2. *Nat Methods*. 2012;9(4):357–9.
29. von Meijenfeldt FAB, Arkhipova K, Cambuy DD, Coutinho FH, Dutilh BE. Robust taxonomic classification of uncharted microbial sequences and bins with CAT and BAT. *Genome Biol*. 2019;20(1):217.
30. Parks DH, Imelfort M, Skennerton CT, Hugenholtz P, Tyson GW. CheckM: assessing the quality of microbial genomes recovered from isolates, single cells, and metagenomes. *Genome Res*. 2015;25(7):1043–55.
31. Tuller T, Felder Y, Kupiec M. Discovering local patterns of co - evolution: computational aspects and biological examples. *BMC Bioinformatics*. 2010;11(1):43.
32. Page AJ, Cummins CA, Hunt M, Wong VK, Reuter S, Holden MTG, et al. Roary: rapid large-scale prokaryote pan genome analysis. *Bioinformatics*. 2015;31(22):3691–3.
33. Katoh K, Standley DM. MAFFT Multiple Sequence Alignment Software Version 7: Improvements in Performance and Usability. *Mol Biol Evol*. 2013;30(4):772–80.
34. Stamatakis A, Aberer AJ, Goll C, Smith SA, Berger SA, Izquierdo-Carrasco F. RAxML-Light: a tool for computing terabyte phylogenies. *Bioinformatics*. 2012;28(15):2064–6.
35. Letunic I, Bork P. Interactive Tree Of Life (iTOL) v5: an online tool for phylogenetic tree display and annotation. *Nucleic Acids Res*. 2021;49(W1):W293–6.
36. Pérez-Carrascal OM, Terrat Y, Giani A, Fortin N, Greer CW, Tomas N, et al. Coherence of *Microcystis* species revealed through population genomics. *ISME J*. 2019;13(12):2887–900.
37. Dick GJ, Duhaime MB, Evans JT, Errera RM, Godwin CM, Kharbush JJ, et al. The genetic and ecophysiological diversity of *Microcystis*. *Environ Microbiol*. 2022;23(12):7278-7313.

38. Blondeau M, Sachse M, Boulogne C, Gillet C, Guigner JM, Skouri-Panet F, et al. Amorphous Calcium Carbonate Granules Form Within an Intracellular Compartment in Calcifying Cyanobacteria. *Front Microbiol.* 2018;9.
39. Mehta N, Gaëtan J, Giura P, Azaïs T, Benzerara K. Detection of biogenic amorphous calcium carbonate (ACC) formed by bacteria using FTIR spectroscopy. *Spectrochim Acta A Mol Biomol Spectrosc.* 2022;121262.
40. Horst GP, Sarnelle O, White JD, Hamilton SK, Kaul RB, Bressie JD. Nitrogen availability increases the toxin quota of a harmful cyanobacterium, *Microcystis aeruginosa*. *Water Res.* 2014;54:188–98.
41. Weyhenmeyer GA, Hartmann J, Hessen DO, Kopáček J, Hejzlar J, Jacquet S, et al. Widespread diminishing anthropogenic effects on calcium in freshwaters. *Sci Rep.* 2019;9(1):10450.
42. Chen H, Lüring M. Calcium promotes formation of large colonies of the cyanobacterium *Microcystis* by enhancing cell-adhesion. *Harmful Algae.* 2020;92:101768.
43. Gu P, Li Q, Zhang W, Zheng Z, Luo X. Effects of different metal ions (Ca, Cu, Pb, Cd) on formation of cyanobacterial blooms. *Ecotoxicol Environ Saf.* 2020;189:109976.
44. Yancey CE, Smith DJ, Den Uyl PA, Mohamed OG, Yu F, Ruberg SA, et al. Metagenomic and Metatranscriptomic Insights into Population Diversity of *Microcystis* Blooms: Spatial and Temporal Dynamics of *mcy* Genotypes, Including a Partial Operon That Can Be Abundant and Expressed. Rudi K, editor. *Appl Environ Microbiol.* 2022;e02464-21.
45. Cao H. Comprehensive and functional analyses reveal the genomic diversity and potential toxicity of *Microcystis*. *Harmful Algae.* 2022;11.

46. Humbert JF, Barbe V, Latifi A, Gugger M, Calteau A, Coursin T, et al. A Tribute to Disorder in the Genome of the Bloom-Forming Freshwater Cyanobacterium *Microcystis aeruginosa*. PLOS ONE. 2013;8(8):e70747.
47. Tanabe Y, Hodoki Y, Sano T, Tada K, Watanabe MM. Adaptation of the Freshwater Bloom-Forming Cyanobacterium *Microcystis aeruginosa* to Brackish Water Is Driven by Recent Horizontal Transfer of Sucrose Genes. Front Microbiol. 2018;9.
48. Chen M, Xu CY, Wang X, Ren CY, Ding J, Li L. Comparative genomics analysis of c-di-GMP metabolism and regulation in *Microcystis aeruginosa*. BMC Genomics. 2020;21(1):217.
49. Humbert JF, Barbe V, Latifi A, Gugger M, Calteau A, Coursin T, et al. A Tribute to Disorder in the Genome of the Bloom-Forming Freshwater Cyanobacterium *Microcystis aeruginosa*. PLOS ONE. 2013;8(8):e70747.
50. Meyer KA, Davis TW, Watson SB, Denef VJ, Berry MA, Dick GJ. Genome sequences of lower Great Lakes *Microcystis* sp. reveal strain-specific genes that are present and expressed in western Lake Erie blooms. Humbert JF, editor. PLOS ONE. 2017;12(10):e0183859.
51. Kurmayer R, Christiansen G, Chorus I. The Abundance of Microcystin-Producing Genotypes Correlates Positively with Colony Size in *Microcystis* sp. and Determines Its Microcystin Net Production in Lake Wannsee. Appl Environ Microbiol. 2003;69(2):787–95.
52. Wang X, Sun M, Xie M, Liu M, Luo L, Li P, et al. Differences in microcystin production and genotype composition among *Microcystis* colonies of different sizes in Lake Taihu. Water Res. 2013;47(15):5659–69.
53. Cosmidis J, Benzerara K. Why do microbes make minerals? Comptes Rendus Géoscience. 2022;354(G1):1–39.

54. Badger MR, Price GD. CO₂ concentrating mechanisms in cyanobacteria: molecular components, their diversity and evolution. *J. Exp. Bot.* 2003;54 (383): 609-622.